Pergamon

Acta mater. Vol. 45, No. 11, pp. 4569–4581, 1997

Printed in Great Britain
PII: S1359-6454(97)00135-3
1359-6454/97 $17.00 + 0.00

CREEP OF METALS CONTAINING HIGH VOLUME FRACTIONS OF UNSHEARABLE DISPERSOIDS—PART I. MODELING THE EFFECT OF DISLOCATION PILE-UPS UPON THE DETACHMENT THRESHOLD STRESS

D. C. DUNAND† and A. M. JANSEN‡

Department of Materials Science and Engineering, Massachusetts Institute of Technology, Cambridge, MA 02139, U.S.A.

(Received 22 November 1996; accepted 24 March 1997)

Abstract—The high creep resistance of dispersion-strengthened metals is the result of a threshold stress, which is determined in existing models by considering the interaction of a single dislocation with dispersoids. This paper presents a new model which takes into account the effect of dislocation pile-ups upon the detachment threshold stress of dispersion-strengthened metals. First, it is shown that dislocation pile-ups are expected to form at dispersoids when the volume fraction and/or size of the dispersoids is large. Then, the equilibrium dislocation positions within the pile-ups are calculated and the resulting shear stress exerted upon the detaching dislocations pinned at the dispersoids is determined. Finally, this pile-up stress is added to the athermal detachment threshold stress determined with existing models to find a total threshold stress. Calculations for aluminum containing 25 vol.% alumina dispersoids show that the magnitude of the pile-up stress is comparable to the athermal threshold stress, and thus contributes significantly to the total threshold stress. The model also predicts a creep activation energy much higher than that of the unreinforced metal as a result of the temperature dependence of the number of dislocations in the pile-ups. © *1997 Acta Metallurgica Inc.*

1. INTRODUCTION

Because of their outstanding strength at elevated temperatures, dispersion-strengthened metals containing unshearable dispersoids have been the subject of many experimental and theoretical creep studies, as reviewed in Refs [1–4]. When deformation is controlled by dislocation glide and climb, the tensile creep rate $\dot{\epsilon}$ of both dispersion-strengthened metals and dispersoid-free metals can be described by a power-law equation:

$$\dot{\epsilon} = A'\sigma^{n'} \exp\left(\frac{-Q'}{RT}\right) \tag{1}$$

where σ is the applied tensile stress, n' the apparent stress exponent, Q' the apparent activation energy, R the gas constant, T the absolute temperature and A is a function of the elastic modulus and temperature. In the low-stress region of the power-law regime, the creep rate of dispersion-strengthened metals is much lower than that of the dispersion-free matrix, while their stress- and temperature sensitivity (n' and Q', respectively) are much higher. This behavior can be modeled by considering an athermal threshold stress σ_{th} below which dislocation creep does not occur, leading to a modified power-law equation:

$$\dot{\epsilon} = A[\sigma - \sigma_{th}]^n \exp\left(\frac{-Q}{RT}\right) \tag{2}$$

where A is a constant proportional to the shear modulus and inversely proportional to temperature, n the matrix stress exponent and Q the matrix activation energy which is equal to the volume diffusion activation energy. While deformation below the athermal threshold stress is possible by thermal activation or by onset of an independent mechanism such as diffusional creep, the athermal threshold stress is a useful approximation allowing a consistent description in the experimentally measured creep range of dispersion-strengthened metals. As reviewed by Refs [1–4] and summarized briefly below, most researchers attribute the power-law threshold stress to the interaction between matrix dislocations and dispersoids.

An upper bound for the threshold stress is given by the Orowan stress σ_{or}, above which dislocations bypass dispersoids by bowing within their glide plane [5]:

$$\sigma_{or} = M \cdot \frac{0.4 \cdot G \cdot b}{\pi \cdot \bar{\lambda}} \cdot \frac{\ln(\bar{d}/b)}{\sqrt{1-\nu}} \tag{3}$$

†Present address: Department of Materials Science and Engineering, Northwestern University, Evanston, IL 60208, U.S.A.
‡Present address: Arthur D. Little, Inc., Cambridge, MA; previously known as A. M. Redsten.

where M is the mean matrix orientation factor, G the matrix shear modulus, ν the matrix Poisson's ratio, b the matrix Burger's vector, $\bar{d} = \sqrt{2/3}d$, the mean diameter of a circular section in a random plane for a spherical particle of diameter d and $\bar{\lambda}$ the mean interparticle distance given by Ref. [5] as

$$\bar{\lambda} = \bar{d}\left(\sqrt{\frac{\pi}{4f}} - 1\right) \tag{4}$$

assuming a cubic arrangement of spherical dispersoids of volume fraction f.

If dislocations can climb out of their glide plane, bypass of the dispersoids (and thus macroscopic creep deformation) can occur at stresses below the Orowan stress. The threshold stress is then the result of the interaction between the dislocations and the dispersoids during the climb bypass. In a first series of models (climb threshold models), the origin of the threshold stress is the increase in dislocation line length during bypass. Thus, the geometric configuration of the dislocation during climb determines the magnitude of the threshold stress. In the local climb model [5–7], the climbing portion of the dislocation assumes the shape of the dispersoid, while in the general climb model [8], the dislocation line between the dispersoids is also allowed to climb out of the slip plane, thus reducing the total dislocation line length. Finally, the cooperative climb model [9] assumes that the dislocation overcomes groups of dispersoids instead of threading between individual dispersoids, further reducing the total dislocation length and the threshold stress.

A second series of models (detachment threshold models) developed by Arzt and coworkers [10, 11] considers the dislocation after it has overcome the dispersoid by climb. If the matrix–dispersoid interface is incoherent, an attractive force resulting from the spreading of the dislocation core pins the dislocation at the departure side of the dispersoid [12]. The resulting detachment threshold stress σ_{det} is given by

$$\sigma_{det} = \zeta\sqrt{1 - k^2}\sigma_{or} \tag{5}$$

where k is the relaxation factor defined as the ratio between the dislocation line energies at the particle–matrix interface and within the bulk matrix. The factor ζ [which is close to unity for low volume fractions f and is then often omitted in equation (5)] is defined as $\zeta = \bar{\lambda}/L$, where L is the center-to-center spacing of spherical dispersoids arranged on a cubic lattice:

$$L = d\left(\frac{\pi}{6f}\right)^{1/3}. \tag{6}$$

While deformation is possible below the detachment threshold stress by thermal activation [13], the resulting creep strain rate is not experimentally measurable if the relaxation factor is less than about $k = 0.9$. Equation (5) can then be considered as the athermal threshold stress for equation (2). As an alternate explanation for the attractive dispersoid–dislocation interaction, Mishra *et al.* [14] considered the dissociation of the climbing lattice dislocation into partial interfacial dislocations. Their model also predicts a threshold stress as a function of dispersoid diameter and volume fraction. Finally, Arzt and Göhring [15] extended the detachment model for the case of a superdislocation in an ordered matrix detaching from a dispersoid, and took into account the additional interactions resulting from the repulsion between the two superpartials and from the attraction owing to the resulting antiphase boundary.

Except for the two models described above where the elastic interaction within a pair of dislocation partials [14] or superpartials [15] is considered, all existing threshold stress models assume that the dislocation overcoming the dispersoid is not affected by the stress field of the other dislocations in the crystal. As described in more detail later, this assumption is adequate for low dispersoid volume fractions typical of most mechanically alloyed or internally oxidized dispersion-strengthened alloys studied to date. Recently, a novel pressure-infiltration casting technique has been developed for fabrication of dispersion-strengthened metals with dispersoid volume fractions (25 vol.% and above) much higher than achievable by mechanical alloying or internal oxidation [16]. As shown by equations (3) and (4), the Orowan stress (and thus the threshold stress and the overall creep resistance of dispersion-strengthened metals) is expected to increase with increasing dispersoid volume fraction. However, for high volume fractions of unshearable dispersoids, the assumption of a single dislocation interacting with a single dispersoid (or dispersoid group) no longer holds, because dislocations are expected to form pile-ups at the dispersoids.

The present paper describes a new model for the detachment threshold stress which takes into account the effect of dislocation pile-ups on the detachment process. The companion article [17] compares the predictions of this model with experimental data on aluminum containing 25 vol.% submicron alumina dispersoids.

2. MODEL

In all existing threshold models, the lattice dislocations are assumed to be randomly distributed in the crystal, so that their stress fields upon the dislocations overcoming the dispersoids are neglected. However, when the number of dispersoids per unit volume is large and when dislocations glide between dispersoids much more rapidly than they

bypass them by climb, dislocation pile-ups can form at dispersoids under the influence of the applied stress, as observed by transmission electron microscopy in a companion article [17]. The resulting spatial distribution of lattice dislocations is no longer random and the stress fields from these pile-ups cannot anymore be assumed to cancel at all points within the material. Rather, these stress fields will affect the lead pile-up dislocation pinned by the dispersoid, and either aid or hinder the bypassing process (bowing, climb or detachment) by which this controlling dislocation overcomes its obstacle, and thus will either decrease or increase the value of the threshold stress.

In the following sections, we model the threshold stress in dispersion-strengthened metals with high volume fractions of dispersoids by first determining the number of dislocations per dispersoids, then calculating their equilibrium positions and finally computing the stress from the pile-ups upon the dislocation controlling the bypass mechanism.

2.1. *Number of dislocations per dispersoid*

Dislocation pile-ups can form at dispersoids if the number N of mobile matrix dislocations of length L per dispersoid is larger than unity. Assuming straight dislocations with density ρ and dispersoids arranged on a cubic lattice, N is the ratio of the number of dislocations [with length L and within a unit matrix volume $(1-f)\rho/L$, where L is given by equation (6)] and the number of dispersoids per unit volume L^3:

$$N = (1-f)\cdot\rho\cdot\left(\frac{\pi}{6\cdot f}\right)^{2/3} d^2. \tag{7}$$

Furthermore, the density of mobile dislocations ρ can be expressed as

$$\rho = \left(\frac{\sigma}{\alpha\cdot G\cdot b}\right)^2 \tag{8}$$

where α is a constant and the applied stress σ is usually a free variable. However, the stress range where dispersion-strengthened metals are typically used for structural applications is bounded by an upper limit, the Orowan stress σ_{or}, and a lower limit, the threshold stress, itself a fraction of the Orowan stress. We thus assume that the applied stress is a constant fraction of the Orowan stress:

$$\sigma = C\cdot\sigma_{Or} \tag{9}$$

where C is a constant less than unity. Insertion of equations (3), (4), (8) and (9) into equation (7) gives an expression for N which is independent of both the dispersoid spacing L and the dispersoid diameter d, except for a weak logarithmic dependence:

$$N = \left[C'\cdot\frac{\sqrt{1-f}}{\sqrt[3]{f}(\sqrt{\pi/f}-2)}\cdot\ln\left(\frac{d}{b}\right)\right]^2. \tag{10}$$

In equation (10), the constant C' contains geometrical and materials parameters:

$$C' = 0.251\cdot\frac{C\cdot M}{\alpha\sqrt{1-\nu}}. \tag{11}$$

Equation (10) is thus a function of the material constants, α, ν and b and the geometrical parameters C and M which do not vary strongly from metal to metal. Thus, to a first approximation, N depends only on the dispersoid volume fraction f and, weakly, on the dispersoid diameter d.

2.2. *Pile-up equilibrium configuration*

With the number of dislocations per dispersoid N defined by equation (10), we assume that these dislocations form a single pile-up against the dispersoid. The position of N edge dislocations within a pile-up of constant length L [center-to-center dispersoid distance, equation (6)] can then be calculated by using a global equilibrium criterion in the simplified geometrical model shown in Fig. 1(a), which assumes that dispersoids form a regular cubic arrangement in the matrix. While solutions for the positions of dislocations within single-ended, stressed pile-ups and within double-ended, unstressed pile-ups of individual dislocations exist [18], we are not aware of solutions for double-ended, stressed pile-ups of dislocations, as in the present problem. We consider a repeating unit cell with $(N+1)$ parallel, coplanar edge dislocations arranged in a pile-up consisting of $(N-1)$ mobile dislocations bound by two immobile dislocations at positions $x_0 = 0$ and $x_N = L$ [Fig. 1(a)]. To avoid inducing a net curvature in the material by repeating unit cells with dislocations of the same sign over long distances along the x-axis, the material is assumed to be formed of regions with positive edge dislocations (such as in Fig. 1) and equivalent regions with negative edge dislocations with the same overall number of dislocations of each sign. The number of dislocations associated with the boundary between these regions is assumed small compared to the number of dislocations within the regions.

Under the influence of a negative applied shear stress $-\tau_a$, the equilibrium positions x_i [for $i = 1$ to $(N-1)$] of the $(N-1)$ mobile dislocations are given by the force equilibrium condition:

$$\sum_{\substack{j=0\\ j\neq i}}^{N} \tau(x_i - x_j; 0) - \tau_a = 0 \tag{12}$$

where the shear stress $\tau(x, y)$ at point (x, y) owing to the stress field of an edge dislocation at the origin is given by [19]:

$$\tau(x; y) = \frac{Gb}{2\pi(1-\nu)}\frac{x(x^2-y^2)}{(x^2+y^2)^2} \tag{13}$$

which simplifies for $y = 0$ (on the glide plane) to:

$$\tau(x) = \frac{Gb}{2\pi(1-\nu)}\frac{1}{x}. \quad (14)$$

Solving the system of $(N-1)$ non-linear equations given by equation (12) with the shear stress given in equation (14) leads to the equilibrium positions of $(N-1)$ dislocations in an isolated pile-up (i.e. $0 < x_i < L$ and $y = 0$). However, the stress fields of all other pile-ups in neighboring cells also influences

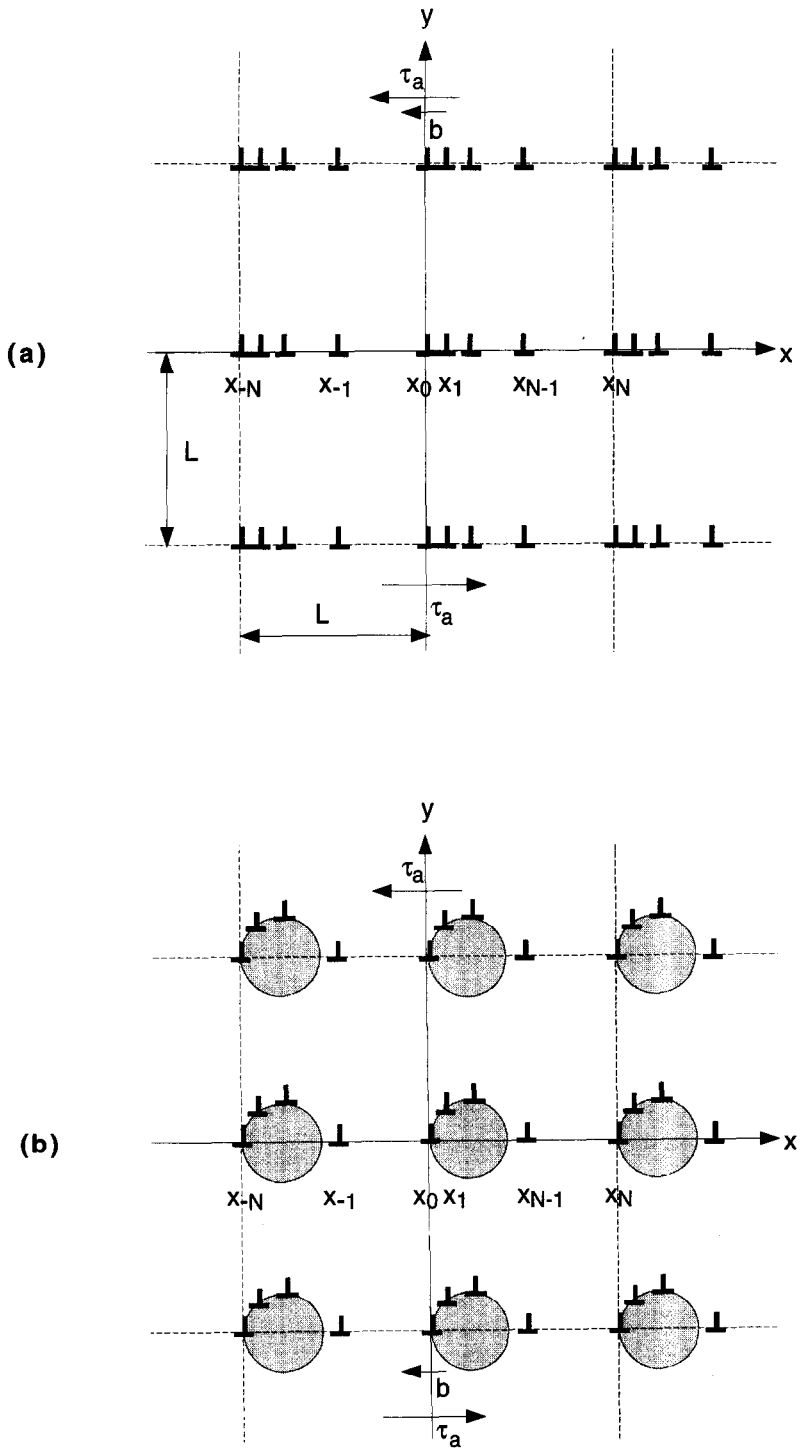

Fig. 1. Two-dimensional view of pile-up configurations. Dislocations at head of pile-ups at $x_{i\cdot N}$ (i: integer) are pinned. (a) Configuration used to find equilibrium dislocation positions; (b) configuration in the presence of dispersoids. For detachment control, the dislocation wall at the origin (x_0) is the reference wall for which the forward stress from walls x_1 to x_{N-1} and the backstress from walls x_{-1} to $x_{-(N-1)}$ are calculated.

the positions of the pile-up dislocations and must be considered in the calculation. A simple approximate solution for this problem is given in the following.

The ensemble of dislocations with the same x-coordinate and the y-coordinate given by $\pm j \cdot L$, where j is a non-zero integer, can be described as a dislocation wall with spacing L [Fig. 1(a)]. The exact solution for the shear stress component at point (x, y) owing to the stress field of an infinite wall of dislocations (with one of its dislocations at the origin) is [20]:

$$\tau(x; y) = \frac{Gb}{2\pi(1-\nu)} \frac{\pi^2 x}{h^2} \frac{\cosh\left(\frac{2\pi x}{h}\right)\cos\left(\frac{2\pi y}{h}\right) - 1}{2\left(\sinh^2\left(\frac{\pi x}{h}\right) + \sin^2\left(\frac{\pi y}{h}\right)\right)^2} \quad (15)$$

where $h = L$ is the spacing of edge dislocations within the wall. For $y = 0$, equation (15) simplifies to

$$\tau(x) = \frac{Gb}{2\pi(1-\nu)} \frac{1}{x} \left(\frac{\pi x}{h}\right)^2 \sinh^{-2}\left(\frac{\pi x}{h}\right). \quad (16)$$

The stress field of the wall [equation (16)] thus corresponds to the stress field of a single dislocation [equation (14)] multiplied by a factor K:

$$K = \left(\frac{\pi x}{h}\right)^2 \sinh^{-2}\left(\frac{\pi x}{h}\right) \quad (17)$$

which tends to unity for small values of x and decays exponentially to zero for positive values of $\pi x/h$. The stress field of a wall is therefore always weaker than that of a single dislocation, as a result of the shielding effect of the dislocations in the wall. Even for short distances, we can neglect the effect upon a given dislocation wall of other walls translated along the x-axis by a factor $\Delta x = \pm j \cdot L$ (where j is a non-zero integer). For example, equation (17) gives a value $K = 7.4 \times 10^{-2}$ for $x = h$ and $K = 5.5 \times 10^{-4}$ for $x = 2h$, corresponding to the first two neighboring walls ($j = 1$–2). For large distances $\pi x/h$, the stress fields of walls on either side of a given dislocation wall are expected to cancel each other. The problem can thus be approximated to finding the equilibrium positions of $(N-1)$ coplanar dislocation walls bound by two immobile walls at $x_0 = 0$ and $x_N = L$. This can be achieved by solving the system of $(N-1)$ equations given by equation (12) with the stress field of walls given in equation (16).

2.3. *Dislocation positions*

Once the x-coordinates of the $(N-1)$ mobile dislocation walls in the pile-up are known, each is assigned a y-coordinate. The simplified geometric model shown in Figs 1(b) and 2 is used with the following assumptions:

- Dislocation detachment from the dispersoid is taken as the controlling mechanism for the motion of dislocations and thus for the material creep. We note that the present model could easily be adapted to other bypassing mechanisms such as local, general or cooperative climb, Orowan bowing or dispersoid shearing. Detachment control is expected for relaxation factors $k < 0.9$ [13] and is thus applicable to many dispersion-strengthened systems of interest such as dispersion-strengthened aluminum or bubble-strengthened tungsten [21]. As noted by Arzt and Rösler [11], the athermal detachment stress [equation (5)] is independent of the dispersoid size or shape (except through the Orowan stress), the height of the intersection between the dispersoid and the glide plane, and the climb process (local, general, cooperative) before the detachment point is reached.
- The material is modeled as a unit cell (shown in Fig. 2) repeating along three orthogonal axes and containing P spherical dispersoids with unbowed edge dislocations on a single glide plane which intersects the dispersoid at its equator. The dispersoids are thus arranged on a cubic lattice and the dislocations form pile-ups on parallel and equidistant glide planes, which are held by the detaching dislocation at the departure side of the dispersoid.
- Dislocations climb cooperatively over groups of dispersoids in the threading shape shown in Fig. 2. This climb geometry is expected for high volume fractions of dispersoids, since it minimizes the dislocation line length [9]. The number of dispersoids being overtaken as a group is the parameter P. The friction stress [10] during glide and climb of the dislocations is neglected, except at the detachment point itself. Friction is expected to be small during cooperative climb.

As shown in Fig. 2, the portion of the dislocation line length that is overcoming the dispersoids (i.e. out of the glide plane) has a length $P \cdot L - (L - d)$. For this portion of the dislocation, the height y_i above the slip plane is determined by the spherical shape of the dispersoid of diameter d:

$$y_i = \tfrac{1}{2}\sqrt{d^2 - (2x_i - d)^2} \quad \text{for} \quad 0 < x_i < d. \quad (18a)$$

For the dislocations which are not in contact with the dispersoid (i.e. still on the slip plane), the height is simply

$$y_i = 0 \quad \text{for} \quad d < x_i < L. \quad (18b)$$

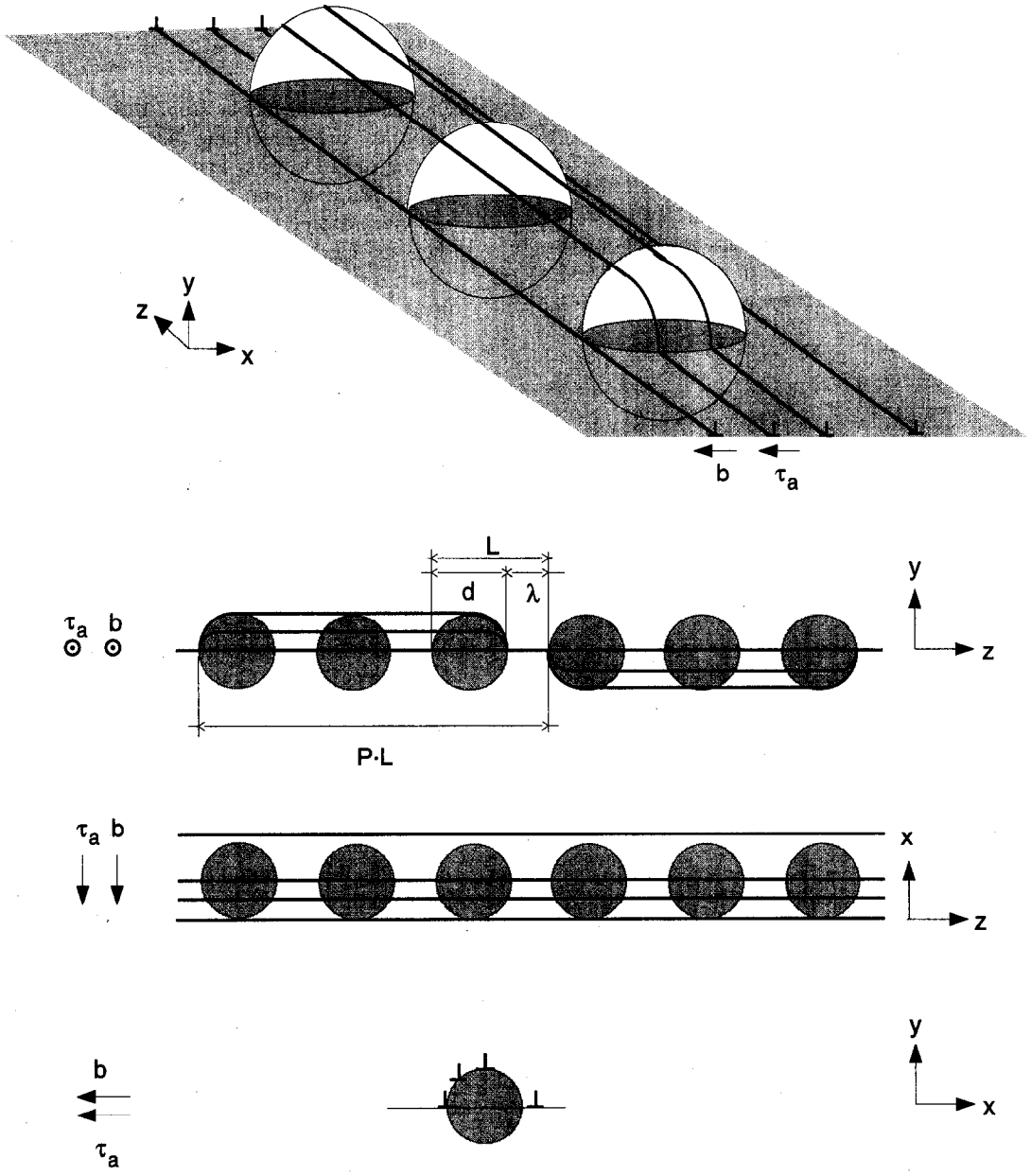

Fig. 2. Three-dimensional view of a unit cell consisting of a dislocation pile-up ($N = 4$) undergoing cooperative climb at groups of dispersoids ($P = 3$); corresponding three orthogonal projections of two unit cells of length $P \cdot L$.

Similarly, the portion of the dislocation of length $(L - d) = \lambda$ which threads along the z-axis between groups of dispersoids is also in the slip plane and has y-coordinate given by

$$y_i = 0 \quad \text{for} \quad 0 < x_i < L. \tag{18c}$$

We thus assume that the x-coordinates of the dislocation segments which have climbed outside the glide plane are unchanged from those calculated within the glide plane from equation (12). This is a simplification, since rearrangement along the x-axis can be expected from the new y-coordinates of the dislocations given by equations (18a)–(18c).

2.4. *Pile-up stress and threshold stress*

Once the coordinates of the dislocations are known, the pile-up stress and the resulting modified threshold stress can be calculated. The following simplifications are made:

- The dispersoids do not affect the elastic stress field of the dislocations. This assumption is correct only if (i) no thermal or elastic mismatch exist between dispersoid and matrix and (ii) if the elastic constants of the dispersoid and matrix are equal. Assumption (i) is expected to be fulfilled at high temperature where mismatch strains can be

relaxed rapidly. Assumption (ii) is not fulfilled in most dispersion-strengthened systems for which a long-range elastic interaction between the matrix dislocation and the dispersoids is expected [22]. This interaction is repulsive (respectively, attractive) for dispersoids stiffer (respectively, less stiff) than the matrix, and is different from the short-range interaction resulting from the relaxation of the dislocation at the interface [12], which is attractive ($k \leqslant 1$) for inclusions both stiffer and less stiff than the matrix.

- The dislocations are straight and parallel both outside and within the glide plane. While the former assumption is expected to hold during cooperative climb, the segments of dislocations that remain in the glide plane ($y = 0$) bow between the dispersoid with a radius inversely proportional to the effective stress. We thus model the elastic interaction between bowed dislocations as equivalent to that between straight dislocations.
- The stress field of the curved dislocation arms (with maximum length $\pi d/4$, Fig. 2) connecting the straight sections within and outside the glide plane is neglected. This assumption becomes better, the larger the number P of dispersoids being cooperatively bypassed.
- Since the stress fields of dislocation walls decay rapidly with distance [equations (16) and (17)], it is sufficient to consider the effect of the two pile ups of $(N-1)$ dislocation walls on either sides of the pinned, detaching dislocation at the origin (Fig. 2).

The pile-up of walls with positions x_{-1} to $x_{-(N-1)}$ exerts on the dislocation pinned at the origin a (usually positive) backstress τ_b which opposes the (negative) applied stress τ_a. By symmetry, this backstress is equal to the stress upon the detaching dislocation at position $x_N = L$ owing to walls at positions x_1 to x_{N-1}:

$$\tau_b = \sum_{i=1}^{N-1} \tau(L - x_i; y_i). \tag{19}$$

On the other hand, the pile-up of walls at positions x_1 to x_{N-1} exerts on the detaching dislocation at the origin a (usually negative) forward stress τ_f which aids the (negative) applied stress τ_a:

$$\tau_f = \sum_{i=1}^{N-1} \tau(-x_i; y_i). \tag{20}$$

Adding the contributions of the forward and backstress (which are usually of opposite signs) gives the total pile-up shear stress τ_p exerted by the two nearest-neighbor pile-ups of walls in the interval $-L < x < L$ upon the pinned dislocation at the origin.

Along the z-axis, the dislocation line is separated into two regions (Fig. 2): the dispersoid region with a line length fraction $1 - (L-d)/P \cdot L$ [where the y-coordinate of the dislocations is given by equations (18a) and (18b)] and the interdispersoid region with a line length fraction $(L-d)/P \cdot L$ [where the y-coordinate of the dislocations is given by equation (18c)]. The net pile-up stress in the interdispersoid region τ_p^i is given by:

$$\tau_p^i = \tau_b^i + \tau_f^i \tag{21}$$

where τ_b^i and τ_f^i are given by equations (19) and (20) with $y = 0$ [equation (19c)]. The pile-up stress τ_p^i in the interdispersoid region is always of the same sign as the applied shear stress (and thus it aids the detachment process), because the magnitude of τ_f^i is always larger than that of τ_b^i, owing to the geometry of the pile-ups. Similarly, the net pile-up stress in the dispersoid region τ_p^p is

$$\tau_p^p = \tau_b^p + \tau_f^p \tag{22}$$

where τ_b^p and τ_f^p are given by equations (19) and (20) with the y-coordinate defined by equations (18a) and (18b). Since the dislocations between $x_o = 0$ and $x = d$ have non-zero y-coordinates [equation (18a)], the sign and magnitude of τ_p^p is sensitive to the exact positions of the dislocations defined by equations (12), (18a) and (18b). Consequently, the pile-up stress τ_p^p in the dispersoid region may be of the same or opposite sign as the applied shear stress, and it may aid or hinder the detachment process.

The total pile-up shear stress on the detaching dislocation at the origin is then taken as the sum of the net pile-up stresses in each region [equations (21) and (22)] weighted by their respective dislocation line length:

$$\tau_p = \frac{(L-d)}{P \cdot L} \tau_p^i + \left[1 - \frac{(L-d)}{P \cdot L}\right] \tau_p^p. \tag{23}$$

Finally, the total tensile threshold stress σ_{th} is the sum of the detachment threshold stress σ_{det} [equation (5)], resulting from the interaction between the detaching dislocation and the dispersoid, and the total pile-up tensile stress $\sigma_p = M \cdot \tau_p$ [equation (23)], resulting from the interaction between the detaching dislocation and the two nearest-neighbor wall pile-ups:

$$\sigma_{th} = \sigma_{det} + \sigma_p. \tag{24}$$

3. DISCUSSION

In the following, we discuss the model presented above and illustrate it by considering the Al–Al_2O_3 system (with materials parameters listed in Table 1), for which experimental data are presented in a companion article [17].

Table 1. Al–Al_2O_3 materials parameters

Property	Value	Ref.
Aluminum matrix		
Magnitude of Burger's vector **b** (nm)	0.286	[23]
Poisson's ratio ν (−)	0.345	[24]
Shear modulus G (GPa)	25.4 [1–0.5 (T − 300)/933]	[23]
Dislocation constant α (−)	1.25	[25]
Mean orientation factor M (−)†	3.06	[24]
Alumina dispersoids		
Volume fraction f (−)	0.25	[16]
Diameter d (nm)	280	[16]
Relaxation parameter with Al k (−)	0.80	[21]

†Randomly oriented f.c.c. metal.

3.1. *Dislocation number*

The number N of dislocations (of length L) per dispersoid is plotted according to equation (10) in Fig. 3 for a range of dispersoid volume fractions f and diameters d and for an applied stress half of the Orowan stress [$C = 0.5$, equation (9)]. We note that equation (10) can only give an estimate for N, as the experimental values for the geometrical and materials parameters α and C are approximate and as dislocation entanglement and curvature may alter the value calculated under the assumption of straight dislocations. Despite the complex volume fraction dependence of equation (10), N is nearly linearly proportional to the volume fraction f in the range $0.01 < f < 0.21$. Furthermore, N slowly increases with increasing dispersoid diameter d. As described in the previous section, pile-ups are expected to form for $N > 1$. Accordingly, the two main dispersoid parameters (diameter d and volume fraction f) are plotted against each other in Fig. 4 for the conditions $N = 1$, $N = 5$ and $N = 10$ [equation (10)]. Most oxide-dispersion-strengthened materials studied in creep to date contain low volume fractions of fine dispersoids (i.e. $f < 0.1$ and $d < 100$ nm), corresponding to a value of N significantly smaller than unity (Figs 3 and 4). For these materials, the influence of neighboring dislocations upon the dislocation overcoming the obstacle can thus be neglected and the models referred to in the Introduction are adequate. However, for dispersion-strengthened materials with high volume fractions of large dispersoids, such as the Al–Al_2O_3 materials investigated in a companion article [17] (i.e. $f = 0.25$ and $d = 280$ nm), equation (10) predicts values of N significantly larger than unity (i.e. $N = 5$). Thus, dislocations may form pile-ups at dispersoids and change the effective shear stress to which the controlling dislocation is subjected, as described in the preceding section. Finally, N is also much larger than unity for materials such as particulate-reinforced metal matrix composites with high volume fractions of very large particles (i.e. $f > 0.1$ and $d > 3\ \mu$m). However, the

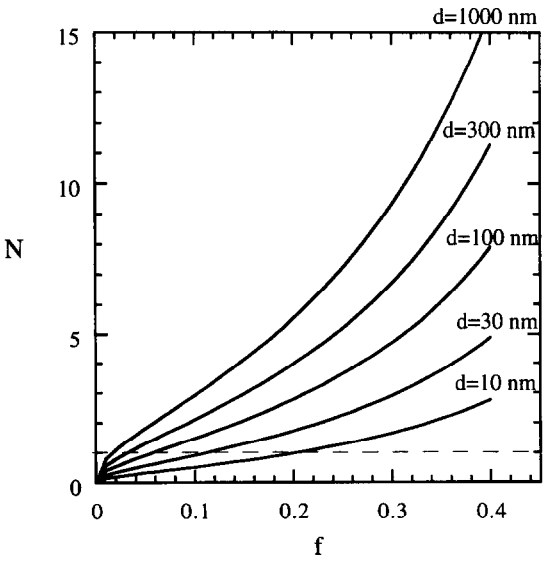

Fig. 3. Number N of dislocations (of length L) per dispersoid as a function of dispersoid volume fraction f and diameter d for a stress half of the Orowan stress ($C = 0.5$) plotted from equation (10).

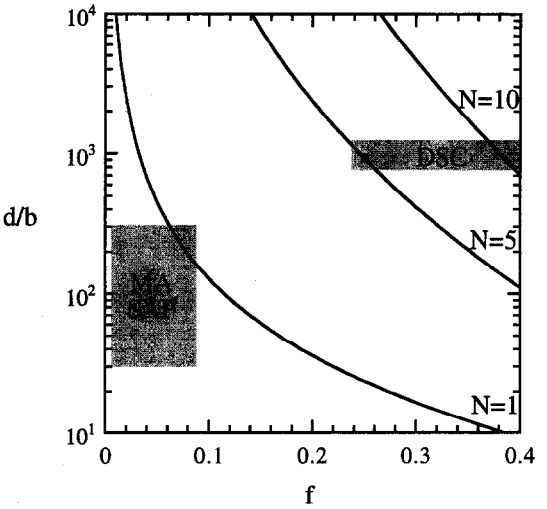

Fig. 4. Dispersoid size d (normalized by matrix Burger's vector **b**) as a function of dispersoid volume fraction f for different values of the number N of dislocations (of length L) per dispersoid. Existing mechanically alloyed (MA) and sintered aluminum powder (SAP) materials typically exhibit values of N less than unity, while dispersion-strengthened cast (DSC) materials discussed in Ref. [17] show values of N significantly higher than unity.

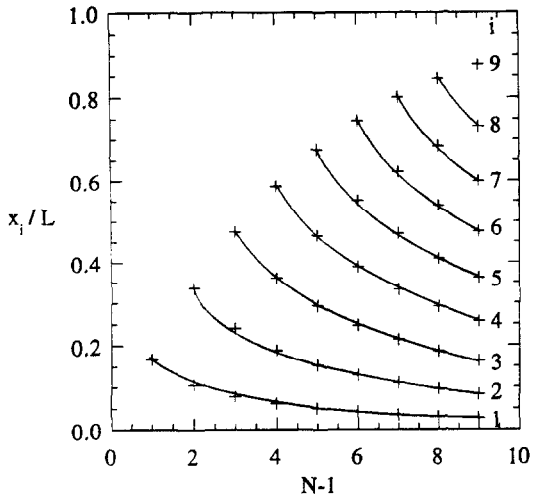

Fig. 5. Dimensionless dislocation position x_i/L as a function of the total number of free dislocations $N-1$ in a pile-up. Positions are calculated from equation (12) for a dislocation pile-up with length $L = 360$ nm [calculated from equation (6) from parameters in Table 1] for dispersion-strengthened aluminum subjected to an applied tensile stress $\sigma = 64$ MPa at a temperature $T = 400$°C. The positions of the pinned dislocations at the head of the pile-up ($x_0/L = 0$) and at its end ($x_N/L = 1$) are not marked. Lines connect the ith dislocations in each pile-up.

magnitude of the Orowan stress for these materials is small, because of the large interparticle distance resulting from the large particle diameter [equations (3) and (4)]. The creep strength of these materials is not dictated by dislocation–dispersoid interactions but by constrained matrix deformation, load transfer from matrix to reinforcement and, at lower temperature, by forest hardening from punched dislocations [16, 26–28]. Therefore, the following discussion concerning the threshold stress does not apply to those materials.

3.2. *Pile-up configuration*

The position along the x-axis of each of the $N-1$ mobile dislocations in the pile-up, as determined numerically from equation (12), is shown in Fig. 5 for dispersion-strengthened aluminum (Table 1) for representative stress and temperature values ($\tau/\mu = 10^{-3}$, $T/T_m = 0.72$). Using the stress field of a wall [equation (16), with $h = L$] resulted in an interdislocation distance slightly smaller than if the stress field of a single, unshielded dislocation [equation (14)] had been used [29]. Varying the applied stress and the temperature within the expected window of use for dispersion-strengthened aluminum has only a small effect on the dislocation positions [29, 30]. As N increases, the interdislocation distance decreases (since the pile-up length L is constant) and the magnitude of the stress from the pile-up dislocations upon both pinned dislocations at the head of the pile up ($x/L = 0$) and at its end ($x/L = 1$) increases. Figure 5 also shows that, with increasing N, the center of gravity of the pile-up moves towards the pinned dislocation at the head of the pile-up, so that the forward stress [equation (20)] increases faster than the backstress [equation (19)].

Finally, we note that the present model can predict unreasonably small interdislocation distances ($\Delta x < b$) for high values of N. This is because an infinite climb resistance is assumed, so that all dislocations are confined to the same glide plane. However, with a high number of dislocations within the pile-up leading to large elastic interactions between neighboring dislocations, dislocations with a small thermally induced offset from the glide plane (jog) in the y-directions can climb rapidly and escape from the pile-up. These dislocations may then form another parallel pile-up against the same dispersoid (a case not treated here) or may join another existing pile-up at another dispersoid, as discussed in more detail in Section 3.4.

3.3. *Threshold stress*

The tensile pile-up stress, calculated numerically from equation (23) with the stress field for walls [equation (15)], is plotted as a function of the number of dislocations in the pile-up in Fig. 6 for different numbers of dispersoids P being cooperatively bypassed and for a range of temperatures and stresses relevant to the experimental data for the Al–Al_2O_3 system presented in the companion article [17]. We discuss here the three general trends apparent from Fig. 6 and give in Ref. [17] a quantitative comparison between model prediction and experimental data.

First, the magnitude of the shear stress upon the detaching dislocation at the origin [equation (15)] is very sensitive to the position of the mobile dislocation walls with $y \neq 0$. This is because the sign of the stress upon the detaching dislocation from each of the climbing, mobile dislocations varies rapidly from positive (attractive interaction for $0 < x_i < d/2$) to negative (repulsive interaction for $d/2 < x_i < d$).

Second, the pile-up stress σ_p increases as P increases, i.e. as the dispersoid climb process becomes more cooperative. For $P = 1$, corresponding to local climb where the dislocation threads between each dispersoid, σ_p is negative because the magnitude of the negative forward stress [equation (20)] is larger than that of the positive backstress [equation (19)]. This is because a large fraction of the dislocation line length ($1 - d/L = 0.22$ for $P = 1$) is in the interdispersoid region where the pile-up stress τ_p^i [equation (21)] has the same sign as the applied shear stress. The detaching dislocation is then subjected to a total negative pile-up stress acting in the direction of the negative applied stress σ and the effective threshold stress [equation (24)] is lower than predicted based solely on the detachment value [equation (5)]. However, climb rather than detachment becomes the controlling threshold mechanism if the effective threshold stress drops below the climb threshold stress (which must also be corrected by considering pile-up stresses). For $P > 1$, σ_p is positive as the

magnitude of the backstress [equation (19)] is larger than that of the forward stress [equation (20)]. Thus, the effective threshold stress is larger than expected from the detachment value, because the detaching dislocation is subjected to a positive total pile-up stress which opposes the negative applied stress.

Third, the pile-up stress is relatively constant for $2 \leqslant N \leqslant 6$ when climb is cooperative ($P > 1$), because, as N increases, the increase in backstress is nearly compensated by an increase in forward stress. For $N > 6$, however, the pile-up stress magnitude increases significantly, while for $N = 1$, the value of the pile-up stress is assumed to be zero, as expected from the symmetry of the model. Finally, for values of N below unity (i.e. volume fractions of fine dispersoids below about 10%, Fig. 4), the stress fields from the individual dislocations are also expected to cancel each other on average, as tacitly assumed in the existing models reviewed in the Introduction.

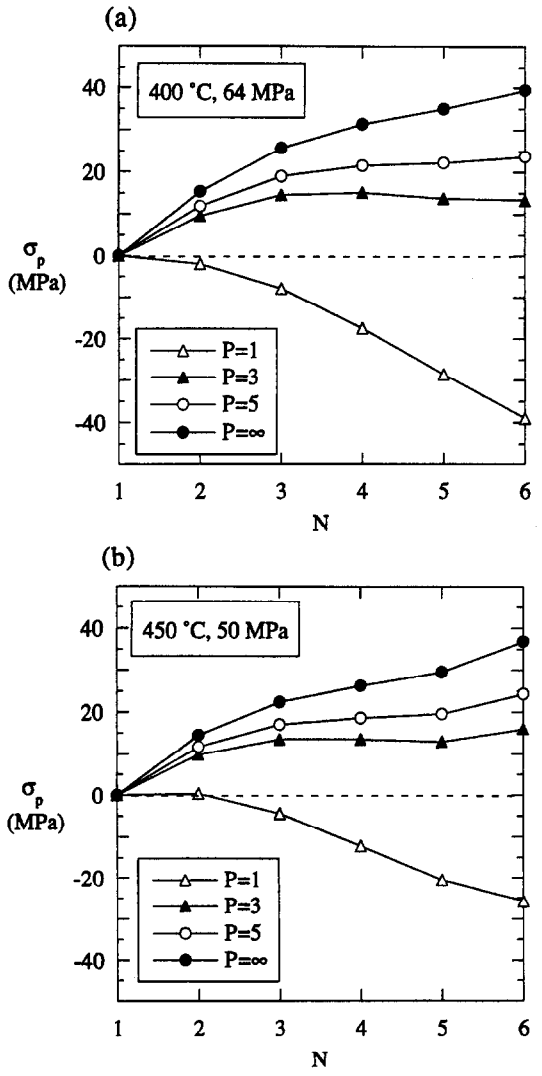

Fig. 6. Tensile pile-up stress σ_p as a function of the number N of dislocations interacting with each dispersoid calculated from equation (23) in dispersion-strengthened aluminum (Table 1). (a) $T = 400°C$, $\sigma = 64$ MPa; (b) $T = 450°C$, $\sigma = 50$ MPa.

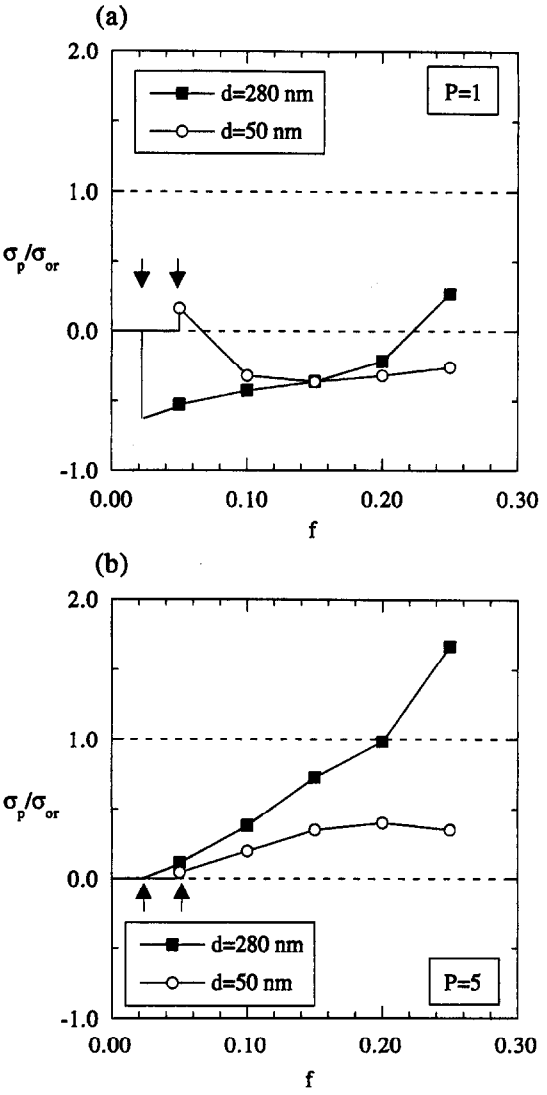

Fig. 7. Pile-up stress (normalized by the Orowan stress) in dispersion-strengthened aluminum (Table 1) as a function of the dispersoid volume fraction f for two values of diameter d at $T = 400°C$ with an applied stress of 60% of the Orowan stress. Arrows indicate the volume fraction f for which the pile-ups contain $N = 1$ dislocation and below which the pile-up stress is zero. (a) Local climb ($P = 1$); (b) cooperative climb ($P = 5$).

Figure 7(a, b) shows the dependence of the pile-up stress σ_p (normalized by the Orowan stress σ_{or}) on the dispersoid volume fraction for dispersoid diameters $d = 0.28$ μm (typical of materials investigated in the companion article [17]) and $d = 50$ nm (typical of SAP and MA materials) at a temperature of 400°C ($T/T_m = 0.72$) and an applied stress $\sigma = 0.6 \cdot \sigma_{or}$. For low volume fractions, the pile-up stress is zero, because N is less than unity. If climb is local [$P = 1$, Fig. 7(a)], the pile-up stress is in the direction of the applied stress (negative values of σ_p/σ_{or}), except for low volume fractions of the fine dispersoids and high volume fractions of the coarse dispersoids. If, as

expected for high dispersoid volume fractions, climb occurs cooperatively over groups of dispersoids [$P = 5$, Fig. 7(b)], the pile-up stress [equation (23)] is positive as it opposes the applied stress and thus increases the effective threshold stress [equation (24)].

The trends in Fig. 7(a, b) are now discussed by examining the factors that influence the number and positions of the pile-up dislocations. For a constant value of σ/σ_{or}, the number N of dislocations (of length L) per dispersoid increases both with increasing volume fraction f and with increasing dispersoid diameter d [equation (10), Figs 3 and 4]. Therefore, for $P > 1$, the magnitude of σ_p/σ_{or} is expected to increase with increasing volume fraction more rapidly for large dispersoids than for small ones. The magnitude of the pile-up stress σ_p is, however, higher for small dispersoids, because the Orowan stress σ_{or} is higher than for larger dispersoids [equation (3)]. Values of σ_p/σ_{or} above unity may not be physically relevant, since, when the effective detachment threshold stress [equation (24)] becomes larger than the threshold stress for bypass by bowing or shearing, these alternate bypass mechanisms control creep. However, the threshold stresses for these mechanisms must also be corrected for the presence of pile-ups, a task which is not attempted in the present paper.

The dispersoid diameter has two further effects upon the dislocation positions and thus the pile-up stress. First, for a given equilibrium x-coordinate [determined for a pile-up of walls in the same glide plane, equations (12) and (16)], the y-coordinate is smaller for fine dispersoids than for large ones [equation (18a)]. Thus, for dislocations with equilibrium positions on the interval $0 < x < d/2$ (which exert an attractive force on the pinned dislocation), this attraction will be larger for fine dispersoids than for coarse ones. Second, the dispersoid diameter determines the number of dislocations with non-zero y-coordinates [equation (18a)]. Since the sign and magnitude of the stress field is sensitive to the value of the y-coordinate, the final pile-up stress can be strongly influenced by the dispersoid size.

3.4. *Activation energy*

Most experimental studies of dispersion-strengthened alloys report an apparent creep activation energy Q' [equation (1)] much larger than the matrix activation energy Q [equation (2)]. The apparent activation energy is defined as

$$Q' = -R\left[\frac{\mathrm{d}(\ln \dot{\epsilon})}{\mathrm{d}(1/T)}\right]_{\sigma = \text{const}} \tag{25}$$

which, using the modified power-law equation (2), gives [2]:

$$Q' = Q - RT + \frac{RT^2}{G}\left(-\frac{\mathrm{d}G}{\mathrm{d}T}\right)(n-1) + \frac{nRT^2}{\sigma - \sigma_{th}}\left(-\frac{\mathrm{d}\sigma_{th}}{\mathrm{d}T}\right) \tag{26}$$

taking into account the temperature dependence of the constant A'. As reviewed in the Introduction, the athermal threshold stress for low dispersoid volume fractions can be expressed as a fraction of the Orowan stress:

$$\sigma_{th} = C_1 \cdot \sigma_{or} \tag{27}$$

where C_1 is a temperature-independent constant less than unity. For example, if the threshold stress is detachment controlled [equation (5)], $C_1 = \zeta(1 - k^2)^{1/2}$. Since the only temperature-dependent term in the Orowan stress [equation (3)] is the shear modulus, it follows from equation (27) that:

$$\frac{1}{\sigma_{th}}\frac{\mathrm{d}\sigma_{th}}{\mathrm{d}T} = \frac{1}{G}\frac{\mathrm{d}G}{\mathrm{d}T}. \tag{28}$$

Introducing equation (28) into equation (26) and rearranging yields:

$$Q' = Q - RT\left[1 + \frac{T}{G}\frac{\mathrm{d}G}{\mathrm{d}T}\left(n\frac{\sigma}{\sigma - \sigma_{th}} - 1\right)\right]. \tag{29}$$

The corrective second term in equation (29) is, however, typically too small to account for the observed discrepancy in activation energy $Q' - Q$, so that a stronger temperature dependence of the threshold stress is often postulated. However, no mechanism for this strong temperature dependence is proposed in existing models, except in a recent paper by Pichler and Arzt [31] who considered jog nucleation with and without thermal activation as the controlling mechanism for dispersoid bypass by climb.

In the present model for dispersion-strengthened metals with $N > 1$, another possible mechanism can be identified. Because both jog nucleation rate and dislocation climb velocity increase with increasing temperature, dislocations within a pile-up will tend to escape the pile-up by climb (as described in Section 3.2) more readily as temperature increases. The total number of dislocations within each pile-up and thus the pile-up stress are then reduced. The magnitude of the total threshold stress [which is the sum of the athermal detachment threshold stress σ_{det} and the pile-up stress σ_p, equation (24)] will then also decrease with increasing temperature. The pile-up stress can also be written as a fraction of the Orowan stress:

$$\sigma_p = C_2 \cdot \sigma_{or}. \tag{30}$$

If C_2 is independent of temperature, the apparent activation energy is given by equation (29). If, however, C_2 is temperature dependent, a new

apparent activation energy Q'' is found by using equations (24) and (30) to evaluate equation (26):

$$Q'' = Q - RT\left[1 + \frac{T}{G}\frac{dG}{dT}\left(n\frac{\sigma}{\sigma - \sigma_{th}} - 1\right)\right] - nRT^2\frac{\sigma_{or}}{\sigma - \sigma_{th}}\frac{dC_2}{dT}. \quad (31)$$

As illustrated in Fig. 7, the constant C_2 (which also depends upon dispersoid geometry and volume fraction, applied stress, etc.) decreases as the number of dislocations in the pile-up decreases. Thus C_2 is also expected to decrease with increasing temperature, so that equation (31) predicts $Q'' > Q'$. Quantitative comparison between equation (31) and experimental data is presented in the companion article [17].

4. SUMMARY

The present paper examines the effect of high volume fractions of dispersoids upon the detachment of dislocations pinned at dispersoids, which often controls the threshold stress and thus the creep properties of dispersion-strengthened alloys, characterized by high stress- and temperature sensitivities of the minimum strain rate.

- When the dispersoid volume fraction is above a critical value, the number N of dislocations interacting with each dispersoid is larger than unity. Dislocation pile-ups are then expected to form at dispersoids, thus affecting the effective shear stress to which the detaching dislocations pinned at the dispersoids are subjected.
- The positions of the dislocations in pile-ups are calculated by considering the equilibrium of walls of dislocations in a repeating unit cell. The shear stress of these dislocations are summed into a pile-up stress acting upon the detaching dislocations at the dispersoid. This pile-up stress is then added to the detachment threshold stress calculated for low volume fractions of dispersoids ($N < 1$).
- The magnitude and sign of the pile-up stress depend upon the number of dislocations in the pile-ups (determined by the dispersoid volume fraction and diameter), the positions of the dislocations within the pile-ups (determined by the dispersoid diameter and shape, the applied stress and the temperature) as well as the number P of dispersoids being bypassed in a cooperative manner (the only adjustable parameter in the model). The effect of these parameters on the threshold stress are illustrated for the Al–Al_2O_3 system, and compared to experimental data in the companion article [17].
- For metals with high volume fractions of dispersoids, the corrected threshold stress is usually higher than predicted by existing models for $N < 1$, valid for low dispersoid volume fractions. Furthermore, the number of dislocations in the pile-up can decrease with increasing temperature, leading to an increase in the temperature dependence of the threshold stress and an increase in the apparent activation energy for creep.

Acknowledgements—This research was supported by the National Science Foundation under grant No. DMR 9417636, with Dr B. McDonald as monitor. The authors also acknowledge the support of the Department of Defense (in the form of a National Defense Science and Engineering Graduate Fellowship for AMJ) and AMAX (in the form of an endowed chair at MIT for DCD).

REFERENCES

1. Gibeling, J. C. and Nix, W. D., *Mater. Sci. Engng*, 1980, **45,** 123.
2. Arzt, E., *Res. Mech.*, 1991, **31,** 399.
3. Raj, S. V., *Mechanical Properties of Metallic Composites*, ed. S. Ochiai. Marcel Dekker, Inc., New York, 1994, p. 97.
4. Arzt, E., *Mechanical Properties of Metallic Composites*, ed. S. Ochiai. Marcel Dekker, Inc., New York, 1994, p. 205.
5. Brown, L. M. and Ham, R. K., *Strengthening Methods in Crystals*, ed. A. Kelly and R. B. Nicholson. Elsevier, Amsterdam, 1971, p. 9.
6. Shewfelt, R. S. W. and Brown, L. M., *Phil. Mag.*, 1974, **30,** 1135.
7. Shewfelt, R. S. W. and Brown, L. M., *Phil. Mag.*, 1977, **35,** 945.
8. Lagneborg, R., *Scripta metall.*, 1973, **7,** 605.
9. McLean, M., *Acta metall.*, 1985, **33,** 545.
10. Arzt, E. and Wilkinson, D. S., *Acta metall.*, 1986, **43,** 1893.
11. Arzt, E. and Rösler, J., *Acta metall.*, 1988, **36,** 1053.
12. Srolovitz, D. J., Luton, M. J., Petkovic-Luton, R., Barnett, D. M. and Nix, W. D., *Acta metall.*, 1984, **32,** 1079.
13. Rösler, J. and Artz, E., *Acta metall. mater.*, 1990, **38,** 671.
14. Mishra, R. S., Nandy, T. K. and Greenwood, G. W., *Phil. Mag.*, 1994, **69A,** 1097.
15. Arzt, E. and Göhring, E., *Scripta metall. mater.*, 1993, **28,** 843.
16. Redsten, A. M., Klier, E. M., Brown, A. M. and Dunand, D. C., *Mater. Sci. Engng*, 1995, **A201,** 88.
17. Jansen, A. M. and Dunand, D. C., *Acta mater.*, 1997, **45,** 4583.
18. Chou, Y. T. and Li, J. C. M., *Mathematical Theory of Dislocations*, ed. T. Mura. The American Society of Mechanical Engineers, New York, 1969, p. 116.
19. Hirth, J. P. and Lothe, J., *Theory of Dislocations, 2nd edn*. John Wiley & Sons, New York, 1982, p. 76.
20. Cottrell, A. H., *Dislocations and Plastic Flow in Crystals*. Clarendon Press, Oxford, 1953, p. 95.
21. Rösler, J., Joos, R. and Arzt, E., *Metall. Trans.*, 1992, **23A,** 1521.
22. Weeks, R. W., Pati, S. R., Ashby, M. F. and Barrand, P., *Acta Metall.*, 1969, **17,** 1403.
23. Frost, H. J. and Ashby, M. F., *Deformation-Mechanism Maps: The Plasticity and Creep of Metals and Ceramics*. Pergamon Press, 1982, p. 21.
24. Meyers, M. A. and Chawla, K. K., *Mechanical Metallurgy: Principles and Applications*. Prentice-Hall, Englewood Cliffs, NJ, 1984, p. 343.
25. Hansen, N., *Acta metall.*, 1977, **25,** 863.

26. Clyne, T. W. and Withers, P. J., *An Introduction to Metal Matrix Composites*. Cambridge University Press, Cambridge, 1993, p. 71.
27. Dunand, D. C. and Derby, B., *Fundamentals of Metal-Matrix Composites*, ed. S. Suresh, A. Mortensen and A. Needleman. Butterworth-Heinemann, Boston, 1993, p. 191.
28. Hutchinson, J. W. and McMeeking, R. M., *Fundamentals of Metal Matrix Composites*, ed. S. Suresh, A. Mortensen, and A. Needleman, Butterworth-Heinemann, Boston, 1993, p. 158.
29. Jansen, A. M., Ph. D. thesis, Massachusetts Institute of Technology, 1996.
30. Jansen, A. M. and Dunand, D. C., *The Johannes Weertman Symposium*, ed. R. J. Arsenault, D. Cole, T. Gross, G. Kostorz, P. K. Liaw, S. Parameswaran and H. Sizek. TMS, Warrendale, 1996, p. 69.
31. Pichler, A. and Arzt, E., *Acta Mater.*, 1996, **44,** 2751.